Renormalization group functions in two-dimensional massive Dirac-like systems near an interface

Alessandra N. Braga,[1,*] Wagner P. Pires,[2,†] Jeferson Danilo L. Silva,[3,‡] Danilo T. Alves,[4,§] and Van Sérgio Alves[4,‖]

[1]*Campus de Ananindeua, Universidade Federal do Pará, 67130-660, Ananindeua, Brazil*
[2]*Instituto de Ciências da Educação, Universidade Federal do Oeste do Pará, 68040-255, Santarém, Brazil*
[3]*Campus Salinópolis, Universidade Federal do Pará, 68721-000, Salinópolis, Brazil*
[4]*Faculdade de Física, Universidade Federal do Pará, 66075-110, Belém, Brazil*

(Received 6 June 2023; accepted 19 December 2023; published 12 January 2024)

In a recent paper [Phys. Rev. D **102**, 016020 (2020)], pseudo quantum electrodynamics was used to simulate the Coulomb interaction between electrons and determine the mass renormalization in a two-dimensional Dirac-like system. In the present paper, we expand upon these findings by examining this system in a certain distance from a planar interface separating two dielectrics. Using the random-phase approximation, we calculate the renormalization group functions and show how the behaviors of the mass, Fermi velocity, and the anomalous dimension of the fermion field are affected by the presence of this interface. To exemplify an application of our formulas, we calculate the influence of this interface on the renormalized energy band gap in a two-dimensional material. In the appropriate limits, our results recover the corresponding ones reported in the aforementioned publication, as well as in others.

DOI: 10.1103/PhysRevD.109.025006

I. INTRODUCTION

Quantum field theory in $2+1$ dimensions has been employed to describe various aspects of high-energy physics, including quark confinement and chiral symmetry breaking [1], as well as condensed matter physics phenomena like the quantum Hall effect and superconductivity [2]. Since the discovery of graphene [3], a two-dimensional material with the thickness of a carbon atom and a massless relativisticlike dispersion relation, numerous attempts have been made to develop theoretical models capable of accurately describing its remarkable properties. Other materials with a honeycomblike lattice, similar to graphene, have gained attention due to their potential technological applications [4]. Silicene, phosphorene, and transitional metal dichalcogenides (TMDs) are examples of such materials that primarily differ from graphene in that their low-energy excitations are, approximately, described by the massive Dirac equation [5].

It is well known that electromagnetic interaction plays an important role in the transport properties of these materials. Studies on graphene reveal that measurement of the renormalization of the Fermi velocity [6], the direct measurement of the dc conductivity [7], and the experimental observation of the fractional quantum Hall effect in ultraclean samples [8] clearly demonstrate that electromagnetic interaction is, in fact, important, at least for a certain temperature scale.

A theoretical model that accurately describes the electronic properties of these materials must account for the fact that electrons and photons exist in different spacetime dimensions. In these materials, electrons exist in $2+1$ dimensions, while photons exist in $3+1$ dimensions. Therefore, constructing a quantum field theory model requires incorporating mixed dimensions. In 1993, Marino proposed a model with these characteristics, which represents QED in $3+1$ projected onto a two-dimensional plane. This theory is known as pseudo quantum electrodynamics (PQED) [9], and it is sometimes referred to as reduced quantum electrodynamics [10].

The PQED model has been demonstrated to exhibit unitarity [11] and causality [12], as well as being scale invariant for a massless theory [13,14]. In addition, it reproduces the static Coulomb potential instead of the peculiar logarithmic one from QED in $2+1$ dimensions. As a result, it has been widely employed with significant success in numerous scenarios involving the aforementioned two-dimensional Dirac-like systems [15–20].

Recently, a branch of PQED that includes effects of boundary conditions imposed by interfaces to the

*alessandrabg@ufpa.br
†wagner.pires@ufopa.edu.br
‡jdanilo@ufpa.br
§danilo@ufpa.br
‖vansergi@ufpa.br

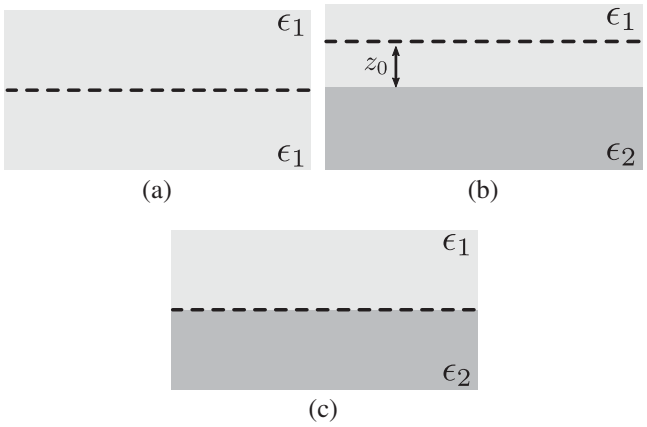

FIG. 1. (a) Illustration of a two-dimensional Dirac-like system (dashed line) embedded in a single medium with dielectric constant ϵ_1. (b) The system is at a distance z_0 to the flat interface between the two dielectrics, with the system being immersed in the medium with dielectric constant ϵ_1. (c) The system is in the flat interface between two media with dielectric constants ϵ_1 and ϵ_2.

electromagnetic field, called cavity PQED, has established that the renormalization of the Fermi velocity and the transport properties of graphene are significantly altered by the presence of a grounded metal plate or a cavity in close proximity to a graphene sheet [18,21,22]. The PQED has also been employed in the random-phase approximation (RPA) to calculate the renormalized mass m (energy band gap) as a function of the carrier concentration n in TMD materials, embedded in a dielectric medium with dielectric constant ϵ_1 [23] [see Fig. 1(a)].

In the present paper, we investigate, in the context of the cavity PQED, the effect of a planar interface, separating two nondispersive semi-infinite dielectrics (ϵ_1 and ϵ_2), on the renormalization of the mass, Fermi velocity, and the anomalous dimension of the fermion field in a planar system located at a distance z_0 from the interface [Fig. 1(b)]. To exemplify an application of our formulas, we calculate the influence of such an interface on the renormalized energy band gap in a two-dimensional material [a monolayer of tungsten diselenide (WSe_2)]. When $\epsilon_1 = \epsilon_2$ [Fig. 1(a)] or $z_0 = 0$ [Fig. 1(c)], the formulas obtained here recover the correspondent ones found in Ref. [23].

This paper is organized as follows. In Sec. II, we present the model and its Feynman rules. In Sec. III, we calculate the photon propagator considering the influence of the dielectrics, and, subsequently, we incorporate the effects of the polarization tensor into this propagator. In Sec. IV, we calculate the electron self-energy at one-loop order in the RPA. In Sec. V, we obtain the renormalization group functions based on the findings from the preceding section, and we derive the renormalization of the mass within the framework of the RPA. In Sec. VI, we discuss some limit cases of the formulas obtained in the preceding section. In Sec. VII, we apply our result to investigate the renormalization of the mass for a monolayer of WSe_2, when this system is situated within a boron nitride substrate, with a distance z_0 separating it from the vacuum interface, or, conversely, when it is located within the vacuum with a distance z_0 from the interface of a boron nitride substrate. Finally, in Sec. VIII, we present our final remarks.

II. THE MODEL AND THE FEYNMAN RULES

The effective theory and complete description in $2+1$ dimensions for electronic systems moving on a plane in vacuum, but interacting as particles in $3+1$ dimensions, is given by [9]

$$\mathcal{L}_{\mathrm{PQED}} = \frac{1}{2}\frac{F_{\mu\nu}F^{\mu\nu}}{(-\Box)^{1/2}} + \mathcal{L}_{\mathrm{D}} + ej^{\mu}A_{\mu} - \frac{\xi}{2}A_{\mu}\frac{\partial^{\mu}\partial^{\nu}}{(-\Box)^{1/2}}A_{\nu}, \quad (1)$$

where $\Box$ is the d'Alembertian operator, $F^{\mu\nu}$ is the usual field intensity tensor of the gauge field A_{μ}, $j^{\mu} = \bar{\psi}\gamma^{\mu}\psi$ is the matter current which is conserved, e is the coupling constant, and we consider $c = \hbar = 1$. To emulate two-dimensional Dirac electrons, we shall consider an anisotropic version of the Dirac Lagrangian given by $\mathcal{L}_{\mathrm{D}} = \bar{\psi}_a(i\gamma^0\partial_0 + iv_F\boldsymbol{\gamma}\cdot\nabla - m)\psi_a$, where v_F is the Fermi velocity, $\bar{\psi}_a = \psi_a^{\dagger}\gamma^0$, $a = 1, \ldots, N$ is a flavor index representing a sum over valleys K and K', γ^{μ} are rank-4 Dirac matrices, $\psi_a^{\dagger} = (\psi^{\star}_{A\uparrow}\psi^{\star}_{A\downarrow}\psi^{\star}_{B\uparrow}\psi^{\star}_{B\downarrow})_a$ is a four-component Dirac spinor representing electrons in sublattices A and B, with different spin orientations, and m represents the bare electron mass. The last term corresponds to the gauge-fixing term. Since the coupling constant is dimensionless, PQED is perturbatively renormalizable according to the power-counting criterion, similar to QED_4. Additionally, it is a unitary [11] and causal [12] theory.

From Eq. (1), one obtains the free photon propagator in Euclidean space:

$$\Delta^{(0)}_{\mu\nu}(k) = \frac{1}{2\sqrt{k^2}}\left[\delta_{\mu\nu} - \left(1 - \frac{1}{\xi}\right)\frac{k_{\mu}k_{\nu}}{k^2}\right], \quad (2)$$

where $k_{\mu} = (k_0, \mathbf{k})$ and $\mathbf{k} = (k_1, k_2)$. In the nonretarded regime, characterized by the consideration of the static limit in the photon propagator, considering the Feynman gauge ($\xi = 1$), it becomes

$$\Delta^{(0)}_{\mu\nu}(k_0 = 0, |\mathbf{k}|) = \frac{1}{2|\mathbf{k}|}\delta_{0\mu}\delta_{0\nu}, \quad (3)$$

which leads to the Coulomb potential for static charges (instead of the peculiar logarithmic one from QED in $2+1$ dimensions) [24]:

$$V(|\mathbf{r}|) = e\int\frac{\mathrm{d}^2\mathbf{k}}{(2\pi)^2}\mathrm{e}^{-i\mathbf{k}\cdot\mathbf{r}}\Delta^{(0)}_{00}(k_0 = 0, |\mathbf{k}|) = \frac{e}{4\pi}\frac{1}{|\mathbf{r}|}. \quad (4)$$

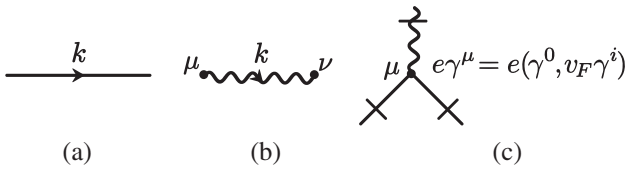

FIG. 2. (a) Electron propagator. (b) Photon propagator. (c) Vertex interaction.

The fermion propagator is

$$S_F^{(0)}(k^\mu) = \frac{k_0\gamma_0 + v_F\mathbf{k}\cdot\boldsymbol{\gamma} + m}{k_0^2 + v_F^2|\mathbf{k}|^2 + m^2}, \tag{5}$$

and the vertex interaction is $\gamma^\mu = (\gamma^0, v_F\gamma^i)$. Feynman rules are depicted in Fig. 2.

In this paper, we consider a planar system in a dielectric medium with dielectric constant ϵ_1. The system is separated by a distance z_0 from a parallel interface with another dielectric medium with dielectric constant ϵ_2 [see Fig. 1(b)].

III. THE PHOTON PROPAGATOR IN THE PRESENCE OF AN INTERFACE BETWEEN TWO DIELECTRICS

Consider an electric charge e in a semi-infinity dielectric medium with dielectric constant ϵ_1 separated by a distance z_0 from the interface between another semi-infinity dielectric medium with dielectric constant ϵ_2. By the image method, the potential V for this configuration at an arbitrary point P (also separated by a distance z_0 from the interface) is (see Fig. 3)

$$V(|\mathbf{r}|) = \frac{1}{4\pi\epsilon_1}\left(\frac{e}{|\mathbf{r}|} + \frac{e'}{|\mathbf{r}'|}\right), \tag{6}$$

where $|\mathbf{r}|$ is the distance between the charge e and the point P and $|\mathbf{r}'|$ is the distance between the image charge e' and the point P. The image charge e' is given by

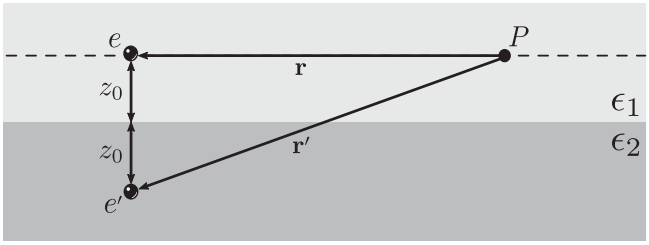

FIG. 3. An electric charge e and its image e', each one separated by a distance z_0 from the interface between the two dielectric media. The charge e is in the medium with dielectric constant ϵ_1, and its image is in the medium with dielectric constant ϵ_2. P is an arbitrary point of the plane that contains the charge e, and it is parallel to the interface.

$$e' = -\frac{\epsilon_2 - \epsilon_1}{\epsilon_2 + \epsilon_1}e, \tag{7}$$

and the distance between the image charge and the point P is $|\mathbf{r}'| = \sqrt{|\mathbf{r}|^2 + 4z_0^2}$. Therefore, the potential at P is

$$V(|\mathbf{r}|) = \frac{e}{4\pi\epsilon_1}\left(\frac{1}{|\mathbf{r}|} - \frac{\kappa_{21}}{\sqrt{|\mathbf{r}|^2 + 4z_0^2}}\right), \tag{8}$$

where we defined

$$\kappa_{21} = \frac{\epsilon_2 - \epsilon_1}{\epsilon_2 + \epsilon_1}. \tag{9}$$

From the static potential (8), we can obtain the photon propagator in the static regime via the inverse Fourier transform (see, for instance, Ref. [24])

$$\Delta_{00}^{(0)}(|\mathbf{k}|) = \frac{1}{e^2}\int \mathrm{d}^2\mathbf{r}e^{-i\mathbf{k}\cdot\mathbf{r}}eV(|\mathbf{r}|), \tag{10}$$

where $k_0 = 0$ and $\mathbf{k}$ and $\mathbf{r}$ are restricted to the plane $z = z_0$; thus, we can write $\mathbf{k}\cdot\mathbf{r} = |\mathbf{k}||\mathbf{r}|\cos\phi$ and $\mathrm{d}^2\mathbf{r} = |\mathbf{r}|\mathrm{d}\phi\mathrm{d}|\mathbf{r}|$. After performing the integration, we obtain

$$\Delta_{00}^{(0)}(|\mathbf{k}|) = \frac{1}{2\epsilon_1|\mathbf{k}|}[1 - \kappa_{21}\exp(-2z_0|\mathbf{k}|)]. \tag{11}$$

The first term represents the propagator in the absence of the medium with ϵ_2 (which corresponds to $z_0 \to \infty$ or $\epsilon_2 \to \epsilon_1$), and the exponential term arises due to the presence of the interface between the two dielectrics. In the following, we shall use this equation to obtain the new expression for the propagator in the large N expansion.

A. Photon propagator in large N expansion

We consider the large N expansion at one-loop order approximation, which is equivalent to the RPA [25,26]. This approximation has been used in the description of some properties of suspended [27,28] and doped [29–31] graphene. It can be conveniently implemented by replacing $e \to e/\sqrt{N}$, for a fixed e.

We will consider the geometric series to calculate the full propagator of the gauge field. Assuming that the interaction vertex is just given by γ_0 (static regime), as illustrated in Fig. 4, we can write

$$\Delta_{00}^{\mathrm{RPA}}(k) = \Delta_{00}^{(0)}(1 - \Pi^{00}\Delta_{00}^{(0)})^{-1}, \tag{12}$$

where [28,32–34]

$$\Pi^{00} = -\frac{e^2}{8}\left[\frac{|\mathbf{k}|^2}{\sqrt{k_0^2 + v_F^2\mathbf{k}^2}} - \frac{4|\mathbf{k}|^2m^2}{(k_0^2 + v_F^2|\mathbf{k}|^2)^{3/2}}\right]. \tag{13}$$

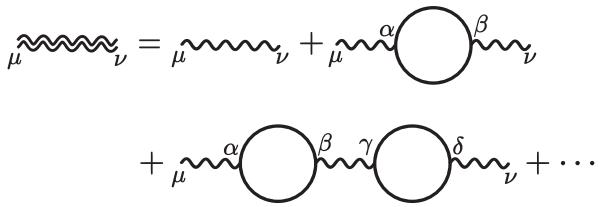

FIG. 4. Gauge field propagator in dominant order in the $1/N$ expansion.

Therefore, we find

$$\Delta_{00}^{\mathrm{RPA}}(k)=\frac{1}{2\epsilon_1|\mathbf{k}|}\left\{\frac{1}{1-\kappa_{21}\exp(-2z_0|\mathbf{k}|)}+\frac{1}{16}\frac{e^2}{\epsilon_1}\times\left[\frac{|\mathbf{k}|}{\sqrt{k_0^2+v_F^2\mathbf{k}^2}}-\frac{4|\mathbf{k}|m^2}{(k_0^2+v_F^2|\mathbf{k}|^2)^{3/2}}\right]\right\}^{-1}. \quad (14)$$

Note that, in the particular case where $\epsilon_1=\epsilon_2$ ($\kappa_{21}=0$) in Eq. (14), our model recovers the case of the full propagator of the gauge field within a single medium [23].

IV. ELECTRON SELF-ENERGY

In this section, we consider the simplest static regime, because it describes well the experimental data [6,35]. This approach, $\gamma^\mu\to\gamma^0$ and $\Delta_{\mu\nu}^{(0)}(k)\to\Delta_{00}^{\mathrm{RPA}}(k_0=0,|\mathbf{k}|)$, has been extensively used in the literature in different contexts and, in particular, in the construction of effective theories that describe two-dimensional materials such as graphene [36] and in the context of the Schwinger-Dyson equations [37–39]. Studies on gauge invariance [40] and Ward identities show that it is preserved in one-loop PQED in the static approximation [41]. In this approximation, the electron self-energy, represented in Fig. 5, reads

$$\Sigma(p)=\frac{e^2}{N}\int\frac{\mathrm{d}^3k}{(2\pi)^3}\gamma_0 S_F^{(0)}(p_\mu-k_\mu)\gamma_0\Delta_{00}^{\mathrm{RPA}}(k). \quad (15)$$

Assuming that the Dirac matrices satisfy $\{\gamma^\mu,\gamma^\nu\}=-2\delta^{\mu\nu}$, $\gamma^0\gamma^0=-\mathbb{I}$, and $\gamma^0\boldsymbol{\gamma}\gamma^0=\boldsymbol{\gamma}$ and performing a power series expansion in the external momentum, we obtain

$$\Sigma(p)=\mathcal{Z}_m+\mathcal{Z}_0\gamma_0 p_0+v_F\mathcal{Z}_1\gamma_i p_i, \quad (16)$$

where the dominant terms are

$$\mathcal{Z}_m=-\frac{e^2}{N}\int\frac{\mathrm{d}^3k}{(2\pi)^3}\frac{m}{k^2+m^2}\Delta_{00}^{\mathrm{RPA}}(k), \quad (17)$$

$$\mathcal{Z}_0=-\frac{e^2}{N}\int\frac{\mathrm{d}^3k}{(2\pi)^3}\frac{v_F^2|\mathbf{k}|^2-k_0^2+m^2}{(k^2+m^2)^2}\Delta_{00}^{\mathrm{RPA}}(k), \quad (18)$$

and

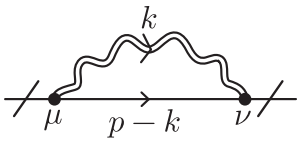

FIG. 5. Electron self-energy diagram.

$$\mathcal{Z}_1=\frac{e^2}{N}\int\frac{\mathrm{d}^3k}{(2\pi)^3}\frac{k_0^2+m^2}{(k^2+m^2)^2}\Delta_{00}^{\mathrm{RPA}}(k). \quad (19)$$

Then, we perform a variable change $v_F k_i\to\bar{k}_i$ in Eq. (16) to spherical coordinates, and the lowest-order terms can be written as

$$\mathcal{Z}_m=-\frac{2\lambda}{\pi^2 N}\int_0^\pi\mathrm{d}\theta\int_0^{\Lambda v_F}k\mathrm{d}k\frac{m}{k^2+m^2}f(k,\theta), \quad (20)$$

$$\mathcal{Z}_0=-\frac{2\lambda}{\pi^2 N}\int_0^\pi\mathrm{d}\theta\int_0^{\Lambda v_F}k\mathrm{d}k\frac{k^2\cos 2\theta+m^2}{(k^2+m^2)^2}f(k,\theta), \quad (21)$$

$$\mathcal{Z}_1=\frac{2\lambda}{\pi^2 N}\int_0^\pi\mathrm{d}\theta\int_0^{\Lambda v_F}k\mathrm{d}k\frac{k^2\cos^2\theta+m^2}{(k^2+m^2)^2}f(k,\theta), \quad (22)$$

where

$$f(k,\theta)=\{[1-\kappa_{21}\exp(-2z_0k\sin\theta/v_F)]^{-1}+\lambda(1-4m^2/k^2)\sin\theta\}^{-1}, \quad (23)$$

$\lambda=e^2/16\epsilon_1 v_F$, and we introduced an ultraviolet cutoff Λv_F in the integrals above (in Sec. VII, where these formulas are applied to a two-dimensional system in condensed matter, this cutoff will be related to the carrier concentration).

V. RENORMALIZATION GROUP FUNCTIONS

The renormalization group equation reads [42,43]

$$\left(\Lambda\frac{\partial}{\partial\Lambda}+\sum_a\beta_a\frac{\partial}{\partial a}-N_F\gamma_\psi-N_{A_\mu}\gamma_{A_\mu}\right)\Gamma^{(N_F,N_{A_\mu})}(p)=0, \quad (24)$$

where, for simplicity, we denote by $\Gamma^{(N_F,N_{A_\mu})}\times(p,e,v_F,m,\Lambda)=\Gamma^{(N_F,N_{A_\mu})}(p)$ the renormalized vertex function with p being the external momenta. Here, $\beta_a=\Lambda(\partial a/\partial\Lambda)$, with $a=\{e,v_F,c,m\}$, are the beta functions of the parameters e, v_F, c, and m. N_F and N_{A_μ} mean the external lines of fermions and A_μ field, respectively. The terms γ_ψ and γ_{A_μ} are the anomalous dimension of the fermion and gauge field, respectively. However, since the polarization tensor for the gauge field is finite at one loop (using the dimensional regularization), we can conclude that $\gamma_{A_\mu}=0$, and, consequently, $\beta_e=\beta_c=0$. Therefore, there is

no renormalization of the speed of light or the electric charge. This is in contrast to the findings of Isobe and Nagaosa in anisotropic QED_4, where both the charge and the speed of light undergo renormalization [44]. Thus, for our purpose, we just need to compute the vertex function for the fermion, and, thus, the renormalization group equation for $\Gamma^{(2,0)}(p)$ becomes

$$\left(\Lambda\frac{\partial}{\partial\Lambda}+\beta_{v_F}\frac{\partial}{\partial v_F}+\beta_m\frac{\partial}{\partial m}-2\gamma_\psi\right)\Gamma^{(2,0)}(p)=0. \quad (25)$$

On the other hand, the vertex function $\Gamma^{(2,0)}(p)$ can be written as

$$\Gamma^{(2,0)}(p)=\gamma_0 p_0+v_F\gamma_i p_i-m+\Sigma(p). \quad (26)$$

Substituting Eq. (26) into (25) and grouping the terms order by order in the $1/N$ expansion, with $\beta_a=N^0\beta_a^{(0)}+(1/N)\beta_a^{(1)}+\cdots$ and $\gamma_\psi=N^0\gamma_\psi^{(0)}+(1/N)\gamma_\psi^{(1)}+\cdots$, we obtain

$$\beta_{v_F}=\frac{v_F\Upsilon}{N}\int_0^\pi d\theta\frac{\Lambda^2v_F^2\sin^2\theta+2m^2}{(\Lambda^2v_F^2+m^2)^2}f(\Lambda v_F,\theta), \quad (27)$$

$$\beta_m=\frac{2m\Upsilon}{N}\int_0^\pi d\theta\frac{\Lambda^2v_F^2\sin^2\theta+m^2}{(\Lambda^2v_F^2+m^2)^2}f(\Lambda v_F,\theta), \quad (28)$$

$$\gamma_\psi=-\frac{\Upsilon}{2N}\int_0^\pi d\theta\frac{\Lambda^2v_F^2\cos 2\theta-m^2}{(\Lambda^2v_F^2+m^2)^2}f(\Lambda v_F,\theta), \quad (29)$$

where we defined $\Upsilon=-2\lambda(\Lambda v_F/\pi)^2$.

For simplicity, we shall consider the small-mass limit ($m^2\ll\Lambda^2v_F^2$) in Eq. (23), which takes the simpler form

$$f(\Lambda v_F,\theta)=\frac{1-\kappa_{21}\exp(-2z_0\Lambda\sin\theta)}{1+\lambda\sin\theta[1-\kappa_{21}\exp(-2z_0\Lambda\sin\theta)]}, \quad (30)$$

and we can neglect the m^2 terms in the integrands of Eqs. (27)–(29). Therefore, from the definitions of β_m and β_{v_F}, we get

$$m=m_0\exp\left[\int_{\Lambda_0}^{\Lambda}\frac{d\Lambda}{\Lambda}C_\lambda(\Lambda)\right] \quad (31)$$

and

$$v_F=v_{0F}\exp\left[\frac{1}{2}\int_{\Lambda_0}^{\Lambda}\frac{d\Lambda}{\Lambda}C_\lambda(\Lambda)\right], \quad (32)$$

where $m_0=m_0(\Lambda_0,\epsilon_1,\epsilon_2,z_0)$ and $v_{0F}=v_{0F}(\Lambda_0,\epsilon_1,\epsilon_2,z_0)$ are reference values of the mass and the Fermi velocity (which must be provided by experiments), respectively, and

$$C_\lambda(\Lambda)=-\frac{4\lambda}{\pi^2N}\int_0^\pi d\theta\sin^2\theta f(\Lambda v_F,\theta). \quad (33)$$

Likewise, in the regime of small mass, the anomalous dimension can be determined as

$$\gamma_\psi=\frac{\lambda}{\pi^2N}\int_0^\pi d\theta\cos(2\theta)f(\Lambda v_F,\theta). \quad (34)$$

Next, we discuss some limit cases of the above formulas.

VI. SOME LIMIT CASES

For $\epsilon_1=\epsilon_2$, Eqs. (30)–(34) recover the corresponding ones found in Ref. [23] and describe the renormalization of the mass, Fermi velocity, and the anomalous dimension for the two-dimensional system in the particular situation illustrated in Fig. 1(a), whereas for $z_0=0$ these formulas describe the situation illustrated in Fig. 1(c).

It is interesting to remark that, even in the limits $\epsilon_1=\epsilon_2$ [Fig. 1(a)] and $z_0=0$ [Fig. 1(c)], the renormalized mass and Fermi velocity depend on the energy scale Λ [23]. In this way, the role of Eqs. (31) and (32) is to reveal how this dependence is affected by an interface [Fig. 1(b)]. On the other hand, in the limits $\epsilon_1=\epsilon_2$ and $z_0=0$, the renormalized anomalous dimension does not depend explicitly on Λ [23]. Thus, the presence of an interface, taken into account in Eq. (34), introduces an explicit dependence on Λ in the renormalized anomalous dimension.

Another interesting limit is to consider $\epsilon_2\gg\epsilon_1=1$ in Eq. (32), which recovers the corresponding result found in Ref. [21], which showed that the renormalization of the Fermi velocity in graphene ($m_0=0$) is inhibited by the presence of a grounded perfectly conducting surface. Adding the limit $z_0\to\infty$, Eq. (32) recovers the corresponding formula found in Ref. [25], which predicted the renormalization of the Fermi velocity in graphene (the experimental observation of such renormalization was reported in Ref. [6]).

VII. APPLICATION

For a two-dimensional system in condensed matter, we can show that the carrier concentration $n=N_e/A$, where N_e is the number of electrons and A is the area occupied by each state, can be written as $n=N_e/A=p_F^2/\pi$ [45,46]. Therefore, it follows that the Fermi momentum reads $p_F=(\pi n)^{1/2}$. This plays the role of our energy scale Λ; thus, we shall use the transformation $\Lambda/\Lambda_0\to(n/n_0)^{1/2}$ for our renormalized functions.

We remark that, for $\epsilon_2=\epsilon_1$ [the situation illustrated in Fig. 1(a)], Eqs. (31) and (33) recover

$$m=m_0\left(\frac{n}{n_0}\right)^{C_\lambda/2}, \quad (35)$$

where

$$C_\lambda = -\frac{1}{\pi^2}\left[4 + \frac{4\cos^{-1}(\lambda)}{\lambda\sqrt{1-\lambda^2}} - \frac{2\pi}{\lambda}\right], \tag{36}$$

found in the literature [23]. For $z_0 = 0$ [situation illustrated in Fig. 1(c)], Eqs. (31) and (33) give Eqs. (35) and (36), with $\epsilon_1 \to (\epsilon_1 + \epsilon_2)/2$.

Theoretical results obtained in Ref. [23], by applying Eq. (35) to tungsten diselenide (WSe_2) [47] and molybdenum disulfide (MoS_2), are in excellent agreement with experimental data [47,48], reinforcing the usefulness of PQED in the study of the electronic properties of these materials. On the other hand, although Eq. (35) can be applied even when the two-dimensional system is in the interface between two dielectrics with dielectric constants ϵ_1 and ϵ_2 [making $\epsilon_1 \to (\epsilon_1+\epsilon_2)/2$ in Eq. (35)], as illustrated in Fig. 1(c), this formula is unable to address the situation where the system is at a distance z_0 from the interface [as illustrated in Fig. 1(b)]. In this case, it is necessary to use the formula (31), obtained in the present paper. Since Eq. (35) is in excellent agreement with experimental data [47,48], an experimental verification of the effects predicted here, according to Eq. (31), seems feasible.

Here, we apply our formulas to investigate the renormalization of the mass for a monolayer of WSe_2, when this system is inside a boron nitride substrate ($\epsilon_1 = 4$), at a distance z_0 from an interface with the vacuum ($\epsilon_2 = 1$) [see Figs. 1(b) and 6]. We also investigate the opposite situation when the monolayer of WSe_2 is inside the vacuum ($\epsilon_1 = 1$), at a distance z_0 from the interface with the boron nitride substrate ($\epsilon_2 = 4$). Taking Refs. [23,47] as basis, we consider the reference values $n_0 = 1.58 \times 10^{12}$ cm^{-2}, $\lambda = 0.48$ (when $\epsilon_1 = 4$), and $\lambda = 1.92$ (when $\epsilon_1 = 1$). Using Eq. (31) and putting the flavor number $N = 2$ due to the degeneracy of the valleys K and K', we obtain the behavior of m/m_0 as a function of n, for several situations discussed next, always comparing our results with those obtained if Eq. (35) (found in Ref. [23]) were applied as if the system were in a single medium ϵ_1.

In Fig. 7(a), we show the ratio m/m_0 versus n, for a monolayer of WSe_2 inside a boron nitride substrate ($\epsilon_1 = 4$), at a distance $z_0 = 100$ nm from an interface with the vacuum. The solid (blue) line shows the curve obtained via Eq. (31), whereas the dashed (orange) line shows the curve obtained via Eq. (35), this latter applied as if the WSe_2

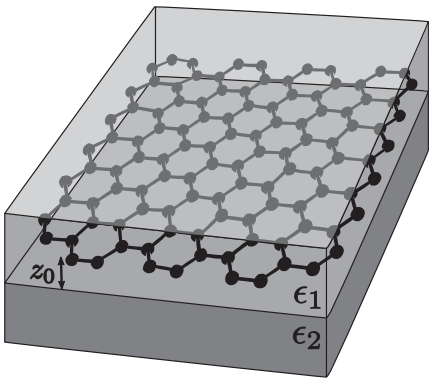

FIG. 6. Illustration of a two-dimensional Dirac-like system parallel and near the interface between two dielectrics with dielectric constants ϵ_1 and ϵ_2. The distance between the material and the interface is z_0, and the two-dimensional system is immersed in the medium with dielectric constant ϵ_1.

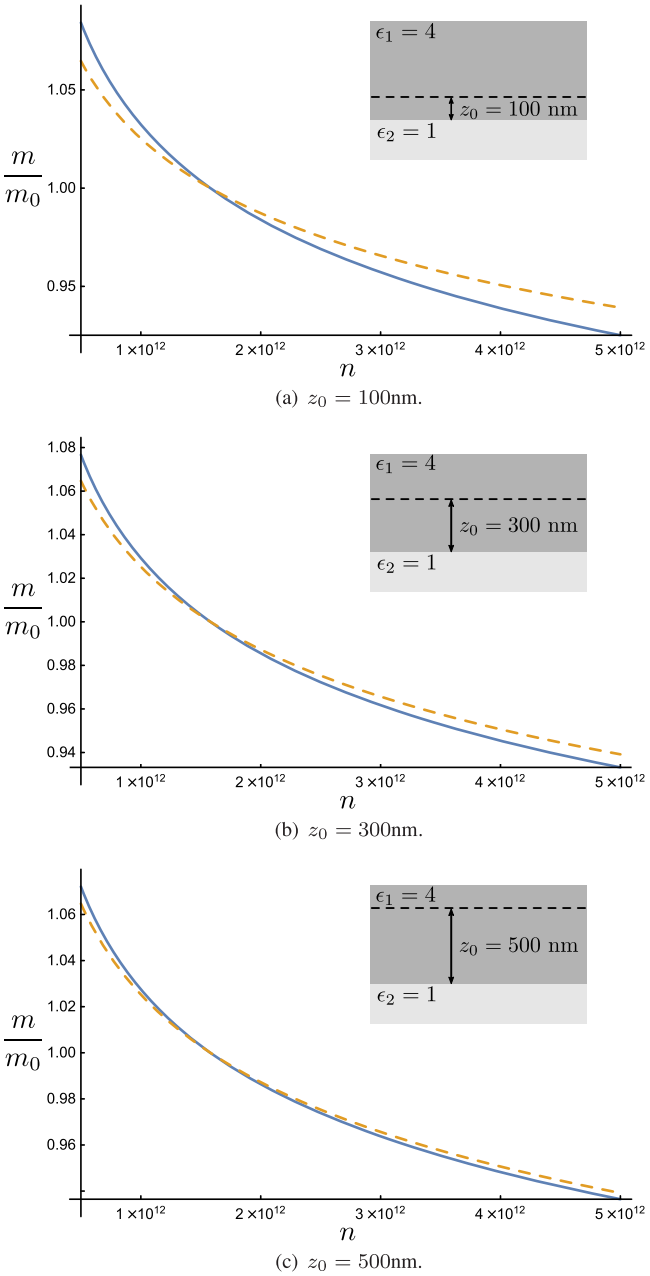

FIG. 7. Ratio m/m_0 as a function of n, for a monolayer of WSe_2 inside a boron nitride substrate ($\epsilon_1 = 4$) near the interface with the vacuum ($\epsilon_2 = 1$), for different values of z_0. The solid (blue) and dashed (orange) lines show the curves obtained via Eqs. (31) and (35), respectively.

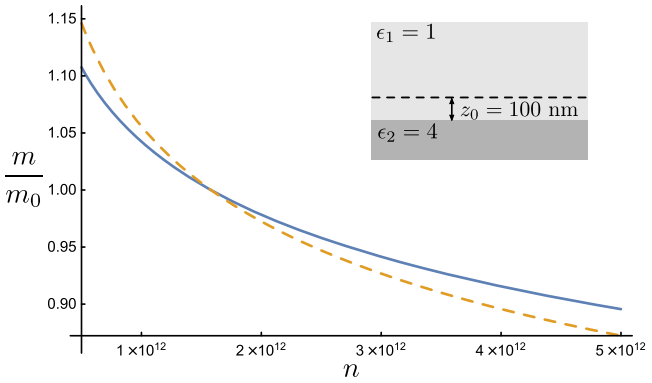

(a) $z_0 = 100$nm.

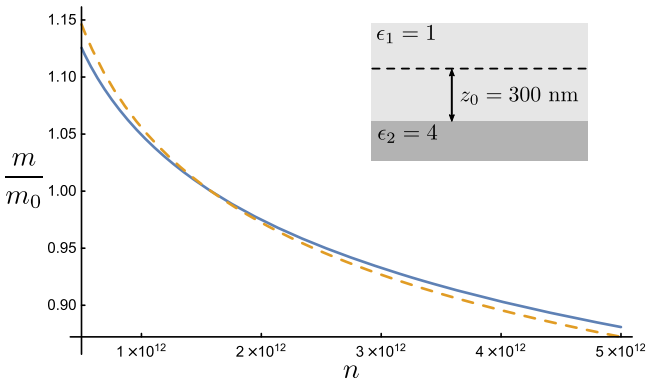

(b) $z_0 = 300$nm.

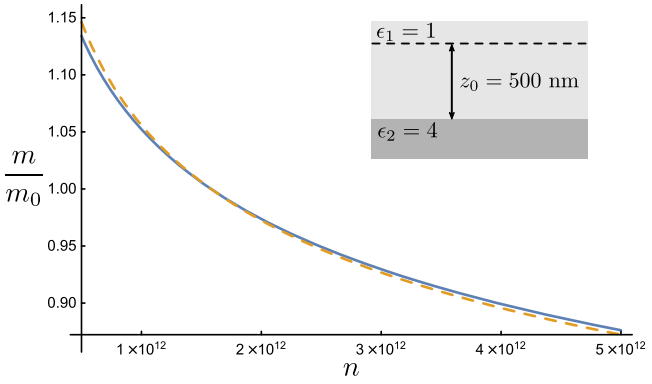

(c) $z_0 = 500$nm.

FIG. 8. Ratio m/m_0 as a function of n in the opposite situation to that shown in Fig. 7. Here, the monolayer of WSe_2 is inside vacuum ($\epsilon_1 = 1$) and near the interface with a boron nitride substrate ($\epsilon_2 = 4$). The solid (blue) and dashed (orange) lines show the curves obtained via Eqs. (31) and (35), respectively.

were immersed in an infinite boron nitride substrate, ignoring the interface with the vacuum. It is evident that Eq. (35) overestimates the values of m/m_0 for $n > n_0$ in comparison to the precise values obtained from Eq. (31), whereas it predicts lower values for $n < n_0$. On the other hand, this difference decreases as z_0 increases, as expected and shown in Figs. 7(b) (for $z_0 = 300$ nm) and 7(c) (for $z_0 = 500$ nm).

In Fig. 8, we show the situation where the media are interchanged, i.e., the monolayer of WSe_2 is inside vacuum ($\epsilon_1 = 1$), at a distance z_0 from the interface with the boron nitride substrate ($\epsilon_2 = 4$). In Fig. 8(a), we show the ratio m/m_0 versus n for $z_0 = 100$ nm. The solid (blue) line shows the curve obtained via Eq. (31), whereas the dashed (orange) line shows the curve obtained via Eq. (35), this latter applied as if the WSe_2 were immersed in an infinite vacuum, ignoring the interface with the boron nitride substrate. One can see that Eq. (35) predicts lower values for m/m_0 in comparison to the precise values obtained from Eq. (31), whereas it predicts higher values for $n < n_0$. On the other hand, this difference decreases as z_0 increases, as expected and shown in Figs. 8(b) (for $z_0 = 300$ nm) and 8(c) (for $z_0 = 500$ nm).

VIII. FINAL REMARKS

We investigated, in the context of the cavity PQED and within the framework of the random-phase approximation, the effect of an interface (between two nondispersive semi-infinite dielectrics) on the renormalization group functions in a two-dimensional Dirac-like system located at a distance z_0 from the interface [Fig. 1(b)]. Our results shown in Eqs. (31)–(34) enable us to predict the behavior of the renormalized mass, Fermi velocity, and the anomalous dimension of the fermion field, under the influence of such an interface.

In the limits $\epsilon_1 = \epsilon_2$ and $z_0 = 0$, Eqs. (30)–(34) recover the corresponding ones found in Ref. [23]. In these limits, the renormalized mass and Fermi velocity continue depending on Λ, but the renormalized anomalous dimension does not. Thus, the role of Eq. (34) is to introduce an explicit dependence on Λ in the renormalized anomalous dimension. For a two-dimensional material, where $p_F = (n\pi)^{1/2}$ assumes the role of the energy scale Λ, Eq. (34) means that, in the presence of an interface, the anomalous dimension of electrons is dependent on the density of states. This result differs from that obtained in Ref. [23], where the anomalous dimension for a two-dimensional material placed on a single substrate does not exhibit such dependence.

In the limit $\epsilon_2 \gg \epsilon_1 = 1$, Eq. (32) recovers the corresponding one found in Ref. [21], which predicts the inhibition of the renormalization of the Fermi velocity in a graphene sheet in the presence of a grounded perfectly conducting surface. Adding the limit $z_0 \to \infty$, Eq. (32) recovers the corresponding formula found in Ref. [25], which predicted the renormalization of the Fermi velocity in graphene. Since this latter prediction was experimentally observed [6], an experimental observation of the renormalization of the Fermi velocity predicted in Eq. (32) seems feasible.

As an application, we considered Eq. (31) to investigate the renormalized mass (band gap) for a monolayer of WSe_2, when this system is inside a boron nitride substrate, at a distance z_0 from an interface with the vacuum (see Fig. 7). We also investigated the opposite situation, when the WSe_2 is inside vacuum, at a distance z_0 from the interface with the boron nitride substrate (see Fig. 8).

We compared our results with those obtained if Eq. (35) (found in Ref. [23]) were applied as if the system were in a single medium. The differences between the more precise predictions, given by our Eq. (31), and those obtained by Eq. (35) are larger for smaller values of z_0 [see Figs. 7(b) and 8(a)], which means that the effect of the interface, captured by Eq. (31), is significant. On the other hand, as z_0 increases, the differences decrease [see Figs. 7(c) and 8(c)], which means that the effect of the interface on the renormalized mass becomes small for larger distances z_0, as expected. Since experiments verifying the dependence of the renormalized mass with the density of states have been made [47,48], an experimental verification of the effects predicted here, according to Eq. (31), seems feasible.

ACKNOWLEDGMENTS

The authors express their gratitude to Leandro O. Nascimento and Luis Fernández for their invaluable contributions and insightful discussions.

[1] P. Maris, Analytic structure of the full fermion propagator in quenched and unquenched QED, Phys. Rev. D **50**, 4189 (1994); T. Appelquist, M. J. Bowick, E. Cohler, and L. C. R. Wijewardhana, Chiral-symmetry breaking in $2+1$ dimensions, Phys. Rev. Lett. **55**, 1715 (1985); C. J. Burden, J. Praschifka, and C. D. Roberts, Photon polarization tensor and gauge dependence in three-dimensional quantum electrodynamics, Phys. Rev. D **46**, 2695 (1992); G. Grignani, G. Semenoff, and P. Sodano, Confinement-deconfinement transition in three-dimensional QED, Phys. Rev. D **53**, 7157 (1996); P. Maris, Confinement and complex singularities in three-dimensional QED, Phys. Rev. D **52**, 6087 (1995).

[2] *The Quantum Hall Effect*, edited by R. E. Prange and S. M. Girvin (Springer, New York, 1990); F. Wilczek, *Fractional Statistics and Anyon Superconductivity* (World scientific, Singapore, 1990), Vol. 5; B. I. Halperin, Quantized Hall conductance, current-carrying edge states, and the existence of extended states in a two-dimensional disordered potential, Phys. Rev. B **25**, 2185 (1982); R. B. Laughlin, Quantized Hall conductivity in two dimensions, Phys. Rev. B **23**, 5632 (1981); R. B. Laughlin, Superconducting ground state of noninteracting particles obeying fractional statistics, Phys. Rev. Lett. **60**, 2677 (1988); Y.-H. Chen, F. Wilczek, E. Witten, and B. I. Halperin, On anyon superconductivity, Int. J. Mod. Phys. B **03**, 1001 (1989).

[3] A. K. Geim and K. S. Novoselov, The rise of graphene, Nat. Mater. **6**, 183 (2007).

[4] B. Radisavljevic, A. Radenovic, J. Brivio, V. Giacometti, and A. Kis, Single-layer MoS2 transistors, Nat. Nanotechnol. **6**, 147 (2011); Q. H. Wang, K. Kalantar-Zadeh, A. Kis, J. N. Coleman, and M. S. Strano, Electronics and optoelectronics of two-dimensional transition metal dichalcogenides, Nat. Nanotechnol. **7**, 699 (2012); H. Liu, A. T. Neal, Z. Zhu, Z. Luo, X. Xu, D. Tománek, and P. D. Ye, Phosphorene: An unexplored 2D semiconductor with a high hole mobility, ACS Nano **8**, 4033 (2014).

[5] A. H. Castro Neto, F. Guinea, N. M. R. Peres, K. S. Novoselov, and A. K. Geim, The electronic properties of graphene, Rev. Mod. Phys. **81**, 109 (2009).

[6] D. C. Elias, R. V. Gorbachev, A. S. Mayorov, S. V. Morozov, A. A. Zhukov, P. Blake, L. A. Ponomarenko, I. V. Grigorieva, K. S. Novoselov, F. Guinea, and A. K. Geim, Dirac cones reshaped by interaction effects in suspended graphene, Nat. Phys. **7**, 701 (2011).

[7] X. Du, I. Skachko, A. Barker, and E. Y. Andrei, Approaching ballistic transport in suspended graphene, Nat. Nanotechnol. **3**, 491 (2008).

[8] X. Du, I. Skachko, F. Duerr, A. Luican, and E. Y. Andrei, Fractional quantum Hall effect and insulating phase of Dirac electrons in graphene, Nature (London) **462**, 192 (2009); K. I. Bolotin, F. Ghahari, M. D. Shulman, H. L. Stormer, and P. Kim, Observation of the fractional quantum Hall effect in graphene, Nature (London) **462**, 196 (2009); F. Ghahari, Y. Zhao, P. Cadden-Zimansky, K. Bolotin, and P. Kim, Measurement of the $\nu = 1/3$ fractional quantum Hall energy gap in suspended graphene, Phys. Rev. Lett. **106**, 046801 (2011); C. R. Dean, A. F. Young, P. Cadden-Zimansky, L. Wang, H. Ren, K. Watanabe, T. Taniguchi, P. Kim, J. Hone, and K. Shepard, Multicomponent fractional quantum Hall effect in graphene, Nat. Phys. **7**, 693 (2011).

[9] E. Marino, Quantum electrodynamics of particles on a plane and the Chern-Simons theory, Nucl. Phys. **B408**, 551 (1993).

[10] E. V. Gorbar, V. P. Gusynin, and V. A. Miransky, Dynamical chiral symmetry breaking on a brane in reduced QED, Phys. Rev. D **64**, 105028 (2001).

[11] E. C. Marino, L. O. Nascimento, V. S. Alves, and C. Morais Smith, Unitarity of theories containing fractional powers of the d'Alembertian operator, Phys. Rev. D **90**, 105003 (2014).

[12] R. L. P. G. do Amaral and E. C. Marino, Canonical quantization of theories containing fractional powers of the d'Alembertian operator, J. Phys. A **25**, 5183 (1992).

[13] D. Dudal, A. J. Mizher, and P. Pais, Exact quantum scale invariance of three-dimensional reduced QED theories, Phys. Rev. D **99**, 045017 (2019).

[14] M. Heydeman, C. B. Jepsen, Z. Ji, and A. Yarom, Renormalization and conformal invariance of non-local quantum electrodynamics, J. High Energy Phys. 08 (2020) 007.

[15] N. Menezes, V. S. Alves, and C. M. Smith, The influence of a weak magnetic field in the renormalization-group functions of $(2+1)$-dimensional Dirac systems, Eur. Phys. J. B **89**, 271 (2016).

[16] N. Menezes, V. S. Alves, E. C. Marino, L. Nascimento, L. O. Nascimento, and C. Morais Smith, Spin g-factor due to

electronic interactions in graphene, Phys. Rev. B **95**, 245138 (2017).
[17] E. C. Marino, L. O. Nascimento, V. S. Alves, N. Menezes, and C. M. Smith, Quantum-electrodynamical approach to the exciton spectrum in transition-metal dichalcogenides, 2D Mater. **5**, 041006 (2018).
[18] D. C. Pedrelli, D. T. Alves, and V. S. Alves, Two-loop photon self-energy in pseudoquantum electrodynamics in the presence of a conducting surface, Phys. Rev. D **102**, 125032 (2020).
[19] E. V. Gorbar, V. P. Gusynin, and M. R. Parymuda, Reduced QED with few planes and fermion gap generation, Entropy **25**, 1317 (2023).
[20] N. Bezerra, V. S. Alves, L. O. Nascimento, and L. Fernández, Effects of the two-dimensional Coulomb interaction in both Fermi velocity and energy gap for Dirac-like electrons at finite temperature, Phys. Rev. D **108**, 056012 (2023).
[21] J. D. L. Silva, A. N. Braga, W. P. Pires, V. S. Alves, D. T. Alves, and E. C. Marino, Inhibition of the fermi velocity renormalization in a graphene sheet by the presence of a conducting plate, Nucl. Phys. **B920**, 221 (2017).
[22] W. P. Pires, J. D. L. Silva, A. N. Braga, V. S. Alves, D. T. Alves, and E. C. Marino, Cavity effects on the Fermi velocity renormalization in a graphene sheet, Nucl. Phys. **B932**, 529 (2018).
[23] L. Fernández, V. S. Alves, L. O. Nascimento, F. Peña, M. Gomes, and E. C. Marino, Renormalization of the band gap in 2D materials through the competition between electromagnetic and four-fermion interactions in large N expansion, Phys. Rev. D **102**, 016020 (2020).
[24] C. D. Roberts and A. G. Williams, Dyson-Schwinger equations and their application to hadronic physics, Prog. Part. Nucl. Phys. **33**, 477 (1994).
[25] M. A. H. Vozmediano and F. Guinea, Effect of Coulomb interactions on the physical observables of graphene, Phys. Scr. **2012**, 014015 (2012).
[26] F. de Juan, A. G. Grushin, and M. A. H. Vozmediano, Renormalization of Coulomb interaction in graphene: Determining observable quantities, Phys. Rev. B **82**, 125409 (2010).
[27] J. González, F. Guinea, and M. A. H. Vozmediano, Marginal-fermi-liquid behavior from two-dimensional Coulomb interaction, Phys. Rev. B **59**, R2474 (1999).
[28] V. N. Kotov, B. Uchoa, and A. H. Castro Neto, $1/N$ expansion in correlated graphene, Phys. Rev. B **80**, 165424 (2009).
[29] S. Das Sarma, E. H. Hwang, and W.-K. Tse, Many-body interaction effects in doped and undoped graphene: Fermi liquid versus non-Fermi liquid, Phys. Rev. B **75**, 121406 (2007).
[30] M. Polini, R. Asgari, Y. Barlas, T. Pereg-Barnea, and A. MacDonald, Graphene: A pseudochiral fermi liquid, Solid State Commun. **143**, 58 (2007).
[31] E. H. Hwang and S. Das Sarma, Dielectric function, screening, and plasmons in two-dimensional graphene, Phys. Rev. B **75**, 205418 (2007).
[32] V. N. Kotov, V. M. Pereira, and B. Uchoa, Polarization charge distribution in gapped graphene: Perturbation theory and exact diagonalization analysis, Phys. Rev. B **78**, 075433 (2008).
[33] R. D. Pisarski, Chiral-symmetry breaking in three-dimensional electrodynamics, Phys. Rev. D **29**, 2423 (1984).
[34] T. W. Appelquist, M. Bowick, D. Karabali, and L. C. R. Wijewardhana, Spontaneous chiral-symmetry breaking in three-dimensional QED, Phys. Rev. D **33**, 3704 (1986).
[35] J. González, F. Guinea, and M. A. H. Vozmediano, Non-Fermi liquid behavior of electrons in the half-filled honeycomb lattice (A renormalization group approach), Nucl. Phys. **B424**, 595 (1994).
[36] E. Barnes, E. H. Hwang, R. E. Throckmorton, and S. Das Sarma, Effective field theory, three-loop perturbative expansion, and their experimental implications in graphene many-body effects, Phys. Rev. B **89**, 235431 (2014).
[37] M. E. Carrington, C. S. Fischer, L. von Smekal, and M. H. Thoma, Role of frequency dependence in dynamical gap generation in graphene, Phys. Rev. B **97**, 115411 (2018).
[38] L. O. Nascimento, V. S. Alves, F. Peña, C. M. Smith, and E. C. Marino, Chiral-symmetry breaking in pseudoquantum electrodynamics at finite temperature, Phys. Rev. D **92**, 025018 (2015).
[39] C. Popovici, C. S. Fischer, and L. von Smekal, Fermi velocity renormalization and dynamical gap generation in graphene, Phys. Rev. B **88**, 205429 (2013).
[40] L. Albino, A. Bashir, A. J. Mizher, and A. Raya, Electron-photon vertex and dynamical chiral symmetry breaking in reduced QED: An advanced study of gauge invariance, Phys. Rev. D **106**, 096007 (2022).
[41] S. Teber and A. Kotikov, Field theoretic renormalization study of interaction corrections to the universal ac conductivity of graphene, J. High Energy Phys. 07 (2018) 082.
[42] S. Weinberg, New approach to the renormalization group, Phys. Rev. D **8**, 3497 (1973).
[43] G. 't Hooft, Dimensional regularization and the renormalization group, Nucl. Phys. **B61**, 455 (1973).
[44] H. Isobe and N. Nagaosa, Renormalization group study of electromagnetic interaction in multi-Dirac-node systems, Phys. Rev. B **87**, 205138 (2013).
[45] E. C. Marino, *Quantum Field Theory Approach to Condensed Matter Physics* (Cambridge University Press, Cambridge, England, 2017).
[46] S. R. A. Salinas, *Introduction to Statistical Physics*, Graduate Texts in Contemporary Physics (Springer, New York, 2013).
[47] P. V. Nguyen, N. C. Teutsch, N. P. Wilson, J. Kahn, X. Xia, A. J. Graham, V. Kandyba, A. Giampietri, A. Barinov, G. C. Constantinescu, N. Yeung, N. D. M. Hine, X. Xu, D. H. Cobden, and N. R. Wilson, Visualizing electrostatic gating effects in two-dimensional heterostructures, Nature (London) **572**, 220 (2019).
[48] F. Liu, M. E. Ziffer, K. R. Hansen, J. Wang, and X. Zhu, Direct determination of band-gap renormalization in the photoexcited monolayer MoS_2, Phys. Rev. Lett. **122**, 246803 (2019).